Open Access   Original Article

Structural biology of HER2/ERBB2 dimerization: mechanistic insights and differential roles in healthy versus cancerous cells

Jayasree Santhanakrishnan[1], Prabhu Meganathan[1*] ⬤, Hemamalini Vedagiri[2] ⬤

[1]Research and Development, Hybrinomics Life Science and Diagnostics LLP, Bangalore 560077, Karnataka, India
[2]Department of Bioinformatics, Bharathiar University, Coimbatore 641046, Tamil Nadu, India

*Correspondence: Prabhu Meganathan, Research and Development, Hybrinomics Life Science and Diagnostics LLP, Bangalore 560077, Karnataka, India. prabmeg@hybrinomics.com

Cite this article: Santhanakrishnan J, Meganathan P, Vedagiri H. Structural biology of HER2/ERBB2 dimerization: mechanistic insights and differential roles in healthy versus cancerous cells. Explor Med. 2024;5:530–43. https://doi.org/10.37349/emed.2024.00237

Abstract

Aim: Present study was done to understand the dimerization of HER2/ERBB2 in normal and cancer cells using in-silico study.

Methods: Pathway analysis was done using Reactome. Structure of HER2/ERBB2 protein was obtained from PDB database, and using Schrödinger software protein structure was analysed and dimerization was done.

Results: In normal cells, HER2/ERBB2 is present at low levels and forms a stable complex with HSP90 (heat shock protein 90), CDC37 (cell division cycle 37), and ERBIN (an adaptor protein of the HER2/ERBB2 receptor). HER2/ERBB2 lacks a ligand-binding site, so it cannot bind ligands to activate HER2/ERBB2 signaling directly. Instead, it heterodimerizes with other EGFR family members, using their ligand-binding sites to activate cell proliferation signaling cascades. In cancer, overexpression of HER2/ERBB2 leads to ligand-independent activation of signaling through dimerization. During this process, HER2/ERBB2 dissociates from the HSP90 complex. Normally, HSP90 helps to correct misfolded and aggregated proteins, but it fails to correct mutated HER2/ERBB2 in cancer cells.

Conclusions: This discussion focuses on the structural changes that HER2/ERBB2 undergoes, particularly in the form of homodimers, under normal and cancerous conditions. This analysis highlights the mutated state of HER2/ERBB2 and the role of HSP90 in this context. Notably, a single-point mutation outside a protein's active site can significantly alter its structure. This is a critical consideration in drug discovery, underscoring the need to evaluate the entire protein conformation during simulations.

Keywords

HER2, ERBB2, HSP90, CDC37, homodimerization

Introduction

HER2/ERBB2 (v-erb-b2 avian erythroblastic leukemia viral oncogene homolog 2), a member of the EGFR (epidermal growth factor receptor) family, comprises four principal domains: (1) an extracellular domain (ECD) that facilitates dimerization on the cell surface; (2) a transmembrane domain (TMD) situated within the lipid bilayer, crucial for receptor activation; (3) a juxtamembrane domain (JMD) in the cytoplasm, linking the TMD and kinase domain; and (4) a kinase domain (KD) in the cytoplasm, responsible for initiating signaling cascades through phosphorylation [1].

HER2/ERBB2 functions as a tyrosine-protein kinase receptor with enzymatic activity in its cytosolic domain. This kinase domain phosphorylates tyrosine residues on target proteins using phosphate groups from ATP hydrolysis. The ATP-binding site and catalytic center within the kinase domain are essential for this phosphorylation process, leading to the activation of cell proliferation signaling cascades [2].

Dimerization of HER2/ERBB2 occurs in the ECD, which is subdivided into four domains: D-I, D-II, D-III, and D-IV. D-I and D-III interact to block ligand binding, while D-II stabilizes protein-protein interactions during dimer formation. The function of D-IV remains less understood [3, 4].

Under normal cellular conditions, HER2/ERBB2 expression is low and stable, forming a complex with HSP90 (heat shock protein 90), CDC37 (cell division cycle 37), and ERBIN (an adaptor protein of the HER2/ERBB2 receptor). HER2/ERBB2 primarily forms heterodimers with other EGFR family members due to its lack of a ligand-binding site, thereby activating downstream signaling [5–7]. However, in cancer, HER2/ERBB2 is overexpressed, leading to homodimer formation and ligand-independent signaling activation. This occurs through dissociation from the HSP90, CDC37, and ERBIN complex [7–9].

Dimer formation results in *trans*-autophosphorylation within the kinase domain, where one kinase domain phosphorylates the tyrosine residues of its partner kinase domain, reciprocally enhancing activation of downstream signaling pathways [10, 11]. This process culminates in the growth factor-independent activation of the RAS/RAF/MAP kinase signaling cascade. Binding of SH1, a signaling adaptor, further recruits the GRB2:SOS1 complex, facilitating RAS guanine nucleotide exchange and subsequently activating the RAS/RAF/MAP kinase cascade (Figure 1) [12, 13]. This pathway has been extensively studied using the Reactome pathway database, providing a comprehensive understanding of HER2/ERBB2's role in cellular signaling and its implications in oncogenesis [14].

HSP90 is a chaperone that ensures protein homeostasis under stress by refolding misfolded and aggregated proteins, while CDC37, a co-chaperone, assists HSP90 in identifying client proteins [15].

In normal cells, HSP90 and CDC37 are secreted under stress conditions, but in cancer cells, where constant stress prevails, these proteins are persistently secreted, facilitating cell proliferation. HSP90 plays a critical role in regulating HER2/ERBB2 activity by binding to a specific loop in its kinase domain, stabilizing and preventing its dimerization, activation, and phosphorylation under normal conditions [7, 9].

In cancer, overexpression of HER2/ERBB2 due to gene amplification disrupts this chaperone binding, promoting HER2/ERBB2-mediated transactivation. HER2/ERBB2 is overexpressed in 15–20% of gastric adenocarcinoma (GC) patients, and while trastuzumab plus chemotherapy is the established first-line treatment, newer therapies like trastuzumab deruxtecan (T-Dxd) are under investigation, with T-Dxd receiving FDA approval in 2021 for advanced GC [16].

LIV-1, a transmembrane protein with zinc transporter and metalloproteinase activity, was initially identified as an estrogen-induced gene in breast cancer and later linked to epithelial-to-mesenchymal transition (EMT). Despite expression variations among cancer subtypes, LIV-1 is moderately to highly expressed in most breast cancers and is targeted by the antibody-drug conjugate (ADC) ladiratuzumab vedotin (SGN-LIV1A), currently in early-phase clinical trials showing promising results as monotherapy or in combination with other treatments [17].

Additionally, hyperglycemia during ipilimumab treatment exacerbates cardiotoxicity and reduces anticancer efficacy in breast cancer cells, a process mediated by the NLRP3 receptor. Combining ipilimumab with empagliflozin or lowering glucose levels mitigates these effects, enhancing treatment response and
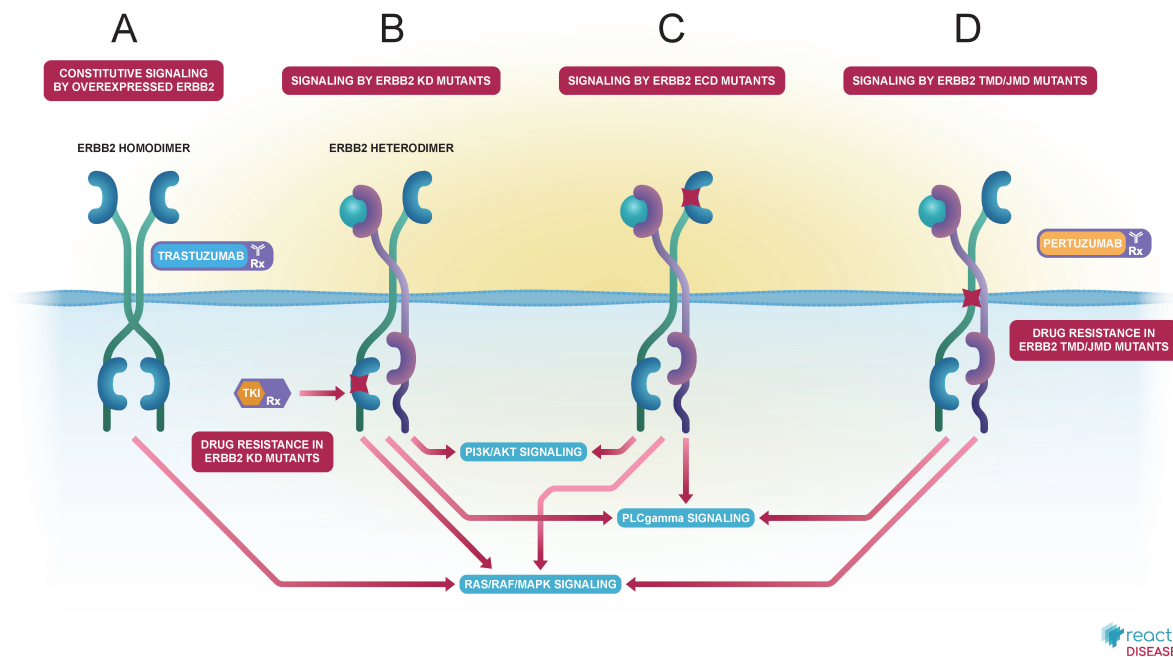
Figure 1. Diagrammatic representation of HER2/ERBB2 dimerizations and their respective activated signaling cascades from Reactome pathway database. (A) Constitutive signaling by overexpressed HER2/ERBB2, where it homodimerizes and activates RAS/RAF/MAPK signaling and also shown, trastuzumab as inhibitor; (B) signaling by HER2/ERBB2 KD mutants, where HER2/ERBB2 heterodimerizes and activates P13/Akt, PLCgamma and RAS/RAF/MAPK signaling and also indicates drug resistance; (C) signaling by HER2/ERBB2 ECD mutants, which heterodimerizes and activates P13/Akt, PLCgamma and RAS/RAF/MAPK signaling; and (D) signaling by HER2/ERBB2 TND/JMD mutants, where it heterodimerizes and activates PLCgamma and RAS/RAF/MAPK signaling and shown pertuzumab as inhibitor, but also drug resistance is shown. ECD: extracellular domain; JMD: juxtamembrane domain; KD: kinase domain; TMD: transmembrane domain

Note. Adapted from "Signaling by ERBB2 in Cancer" by Reactome; c2024 (https://reactome.org/content/detail/R-HSA-1227990). CC BY.

reducing cardiotoxicity. This is the first evidence that hyperglycemia worsens ipilimumab's side effects and efficacy in MCF-7 and MDA-MB-231 cells [18].

The stability of HER2/ERBB2 is critically dependent on HSP90, primarily due to interactions within the kinase domain. This study focuses on the structural and sequential changes in HER2/ERBB2 between normal and cancer cells, emphasizing the mechanism of HER2/ERBB2 homodimerization and the role of HSP90. Understanding the dissociation of HSP90 from the HER2/ERBB2 complex during homodimerization in cancer cells, compared to its stable association in normal cells, is crucial for advancing targeted cancer therapies.

Materials and methods

Pathway analysis

Using the Reactome pathway database (https://reactome.org/), the comprehensive cellular roles of HSP90 were analyzed, including its involvement in autophagy, cell cycle regulation, cellular responses to stimuli, disease processes (particularly cancer), immune system function, programmed cell death, and signal transduction [14]. Specifically, the role of HSP90 in HER2/ERBB2 homodimerization and its contribution to constitutive signaling by overexpressed HER2/ERBB2 was examined. This pathway involves the activation of the RAS/RAF/MAP kinase cascade through interactions with the SH1 domain and the GRB2:SOS1 complex.

Structure retrieval and HER2/ERBB2 homodimerization

X-ray crystal structures of HER2/ERBB2 with high resolution and validation were retrieved from the Protein Data Bank (PDB) (https://www.rcsb.org/). For normal cell HER2/ERBB2, PDB ID 2A91 was used, while for cancer cell ERBB2, PDB ID 3WLW was selected [19]. The homodimer interactions of HER2/ERBB2 in both normal and cancerous conditions were studied using Schrödinger software (Schrödinger Release 2023-4: BioLuminate, Schrödinger, LLC, New York, NY, 2023) [20–22].

In Schrödinger, both PDB structures were prepared and refined using the Protein Preparation Wizard, with parameters adjusted according to the specific requirements of the protein structures (Protein Preparation Wizard; Epik; Impact; Prime, Schrödinger, LLC, New York, NY, 2023) [23]. The homodimerization of HER2/ERBB2 structures was then performed using the protein-protein docking suite, and the docking results were analyzed based on the best PIPER scores [24–26].

Structural and sequential comparative analysis

FASTA files of both normal and cancerous ERBB2 were retrieved from the PDB and aligned using the Smith-Waterman algorithm via local alignment tools BLASTP (https://blast.ncbi.nlm.nih.gov/Blast.cgi) and EMBOSS WATER (https://www.ebi.ac.uk/jdispatcher/psa/emboss_water). Sequential comparison was performed based on identity, similarity, and gap scores [27, 28].

Secondary structure prediction of both HER2/ERBB2 forms was conducted using PSIPRED (http://bioinf.cs.ucl.ac.uk/psipred/), which employs color patterns to differentiate between strands, helices, and coils based on the provided FASTA sequences [29].

Lastly, a comparative analysis of the 3D structures of normal and cancerous HER2/ERBB2, retrieved from PDB, was performed using UCSF Chimera software (https://www.rbvi.ucsf.edu/chimera). This involved superposing the structures to analyze differences and similarities in spatial conformation [30].

Results

Pathway analysis using Reactome pathway database

In aggrephagy, misfolded and aggregated proteins are targeted for degradation through ubiquitination, a process facilitated by HSP90. During this process, misfolded proteins are tagged with ubiquitin, allowing HSP90 to recognize and either refold or eliminate them. Subsequently, the HSP90 complex dissociates after addressing the misfolded proteins (see also Figure S1) [31].

In the cell cycle, HSP90 stabilizes newly synthesized proteins to ensure proper cellular function by forming a complex with FKBPL, which is responsible for protein stability, and CDKN1A, a cell cycle inhibitor. This complex also plays a crucial role in correcting DNA damage to prevent the formation of defective cells, and if the damage cannot be corrected, it leads to apoptosis, thereby conferring resistance to toxicity (see Figure S2) [32–34].

In response to external stimuli, HSF1 is normally present in an inactive state complexed with HSP90. External stresses such as heat, hypoxia, cellular senescence, or an increased amount of unfolded protein in the cell trigger the dissociation of this complex (see Figure S3). Following dissociation, HSF1 activates transcription factors involved in gene expression, which helps regulate stress conditions within the cell [35].

In the immune system, during viral infection, cytosolic viral RNA activates mitochondrial antiviral-signaling protein (MAVS), leading to the formation of the MAVS signalosome. Activated MAVS recruits TANK-binding kinase 1 (TBK1), interferon regulatory factor 3 (IRF3), and IRF7 to the mitochondria, resulting in the activation of IRF3/IRF7 and the subsequent production of type I interferons. Both TBK1 and IRF3 are associated with HSP90, which facilitates signal transduction from TBK1 to IRF3 in infected cells [36].

TOMM70, located on the outer mitochondrial membrane, mediates the translocation of mitochondrial protein precursors from the cytosol into the mitochondria. Molecular chaperone complexes of HSP90 and HSP70 deliver these precursor proteins to TOMM70 for import (see Figure S4). HSP90 forms a complex with TBK1 and IRF3 in the cytosol, delivering them to the MAVS signalosome on the mitochondria, thereby inducing the IRF3-mediated host antiviral response [37, 38].

In programmed cell death, HSP90 participates in regulated necrosis by forming a complex with CDC37. The pseudokinase mixed lineage kinase domain-like protein (MLKL), the terminal effector in the necroptosis pathway, is activated through phosphorylation by receptor-interacting protein kinase-3 (RIPK3). Once activated, MLKL translocates to cellular membranes, causing membrane destabilization and

subsequent cell death. HSP90 and CDC37 together form a complex with MLKL, facilitating its activation (see Figure S5) [39–41].

Similarly, the activation of RIPK3, following the induction of necroptosis, requires the activity of the HSP90-CDC37 complex. This complex physically associates with RIPK3, playing a critical role in regulating necrosis (see Figure S5) [42].

In cancer cell signaling, the association or dissociation of HSP90 with members of the EGFR family (EGFR, ERBB1, ERBB2, ERBB3, and ERBB4) modulates the activation of growth and cell proliferation signaling cascades, including RAS/RAF/MAP kinase, Akt signaling, and DAG/IP3 signaling pathways. When HSP90 associates with these complexes (see Figure S6), it facilitates the loading of client kinases onto EGFR family members. Conversely, upon dissociation, it allows the EGFR members to dimerize (see Figure S7), leading to the activation of signaling cascades through a continuous series of tyrosine residue phosphorylations.

Retrieval of the PDB structures of HER2/ERBB2

The structures of normal and cancer cell HER2/ERBB2 were retrieved from the PDB based on literature references, selecting entries with the highest resolution (< 3 Å) and optimal PDB validation reports for a detailed understanding of their X-ray crystal structures. For normal cell HER2/ERBB2, PDB ID 2A91 was used, while for cancer cell HER2/ERBB2, PDB ID 3WLW was chosen. The retrieved PDB structures of both forms of HER2/ERBB2 are depicted in Figure 2.
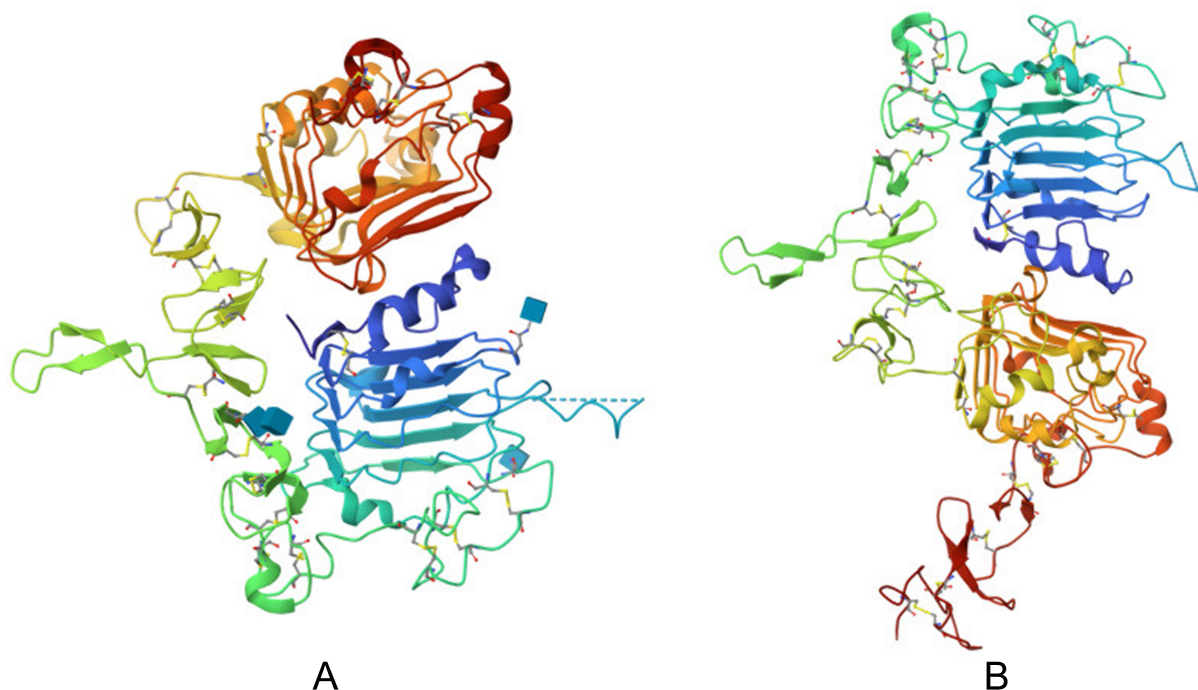
Figure 2. Protein structure of HER2/ERBB2. (A) PDB structure retrieved for normal cell HER2/ERBB2 (PDB ID 2A91); and (B) PDB structure retrieved for cancer cell HER2/ERBB2 (PDB ID 3WLW)
Note. Figure 2A adapted from the RCSB PDB (RCSB.org) of PDB ID 2A91 (Garrett TP, McKern NM, Lou M, Elleman TC, Adams TE, Lovrecz GO, et al. The crystal structure of a truncated HER2/ERBB2 ectodomain reveals an active conformation, poised to interact with other HER2/ERBB2 receptors. Mol Cell. 2003;11:495–505). CC0. Figure 2B adapted from the RCSB PDB (RCSB.org) of PDB ID 3WLW (Hu S, Sun Y, Meng Y, Wang X, Yang W, Fu W, et al. Molecular architecture of the ErbB2 extracellular domain homodimer. Oncotarget. 2015;6:1695–706). CC0.

Dimerization of HER2/ERBB2 structures

Upon homodimerizing the normal cell HER2/ERBB2 structures (PDB ID 2A91) using Schrödinger software, 12 dimerized structures were generated, none of which were stable. A PIPER energy score above –900 is considered indicative of a strong docking interaction, but no such scores were achieved, indicating weak interactions between the normal cell ERBB2 homodimers. The most stable structure identified was POSE2

(Figure 3A), with a PIPER pose energy of –133.7 and PIPER pose score of –71.382 as shown in Table 1. This homodimer exhibited only 12 interacting residues (Figure 3B), preventing a comprehensive interaction analysis in Schrödinger software due to the lack of solid interactions. Consequently, it was determined that normal HER2/ERBB2 cannot form a stable homodimer.

Figure 3. Dimerization of normal HER2/ERBB2. (A) Dimerized structure of normal cell HER2/ERBB2 (PDB ID 2A91) – POSE 2 (using Schrödinger Release 2023-4: BioLuminate, Schrödinger, LLC, New York, NY, 2023); and (B) record of interacting residues in normal cell HER2/ERBB2 dimer noted from Schrödinger software, where blue coloured residues indicate interacting residues

Table 1. PIPER results of dimerized normal HER2/ERBB2 structure (PDB ID 2A91) showing unstable dimer values (using Schrödinger Release 2023-4: BioLuminate, Schrödinger, LLC, New York, NY, 2023)

Title	PIPER pose energy	PIPER pose score	PIPER model number	PIPER cluster size
POSE1	–93.038	–74.6	272	260
POSE2	–133.7	–71.382	21	228
POSE3	–55.632	–106.158	975	145
POSE4	–55.871	–10.35	961	68
POSE5	–55.752	–12.125	966	63
POSE6	–62.301	–54.411	792	59
POSE7	–62.404	–27.389	790	52
POSE8	–60.198	–66.592	847	42
POSE9	–59.333	–32.963	870	40
POSE10	–70.686	–28.635	603	37
POSE11	–59.265	0	871	3
POSE12	–56.614	0	934	3

Homodimerization of cancer cell HER2/ERBB2 (PDB ID 3WLW) resulted in 15 stable dimer structures, all exhibiting PIPER pose energy scores above –900, indicative of strong interactions (Table 2). The most stable interaction was observed in POSE1, with a PIPER pose energy of –1,238.94. The best stable POSE1 homodimer structure is depicted in Figure 4A. Further interaction analysis using Schrödinger software revealed a total of 165 strong to very strong interacting residues, as detailed in Figure 4B and Figure S8. These findings demonstrate that HER2/ERBB2 in cancer cells forms a stable homodimer with robust interactions, leading to the continuous activation of cell proliferation signaling cascades, thereby rapidly increasing cell population.

Table 2. PIPER results of dimerized cancer HER2/ERBB2 structure (PDB ID 3WLW) showing stable dimer values (using Schrödinger Release 2023-4: BioLuminate, Schrödinger, LLC, New York, NY, 2023)

| Title	PIPER pose energy	PIPER pose score	PIPER model number	PIPER cluster size
POSE1	−1,238.94	−192.131	50	93
POSE2	−1,099.976	−481.194	251	90
POSE3	−1,075.053	90.941	341	77
POSE4	−1,234.521	288.706	53	51
POSE5	−967.27	−65.814	969	50
POSE6	−1,162.564	−34.34	139	45
POSE7	−1,132.691	−130.897	187	40
POSE8	−965.985	−119.112	984	35
POSE9	−1,156.086	307.185	141	33
POSE10	−1,212.369	−80.513	73	32
POSE11	−1,083.691	−10.777	297	32
POSE12	−974.888	43.566	899	32
POSE13	−1,006.026	−18.822	683	31
POSE14	−1,041.641	142.197	479	29
POSE15	−1,041.1	61.322	483	24
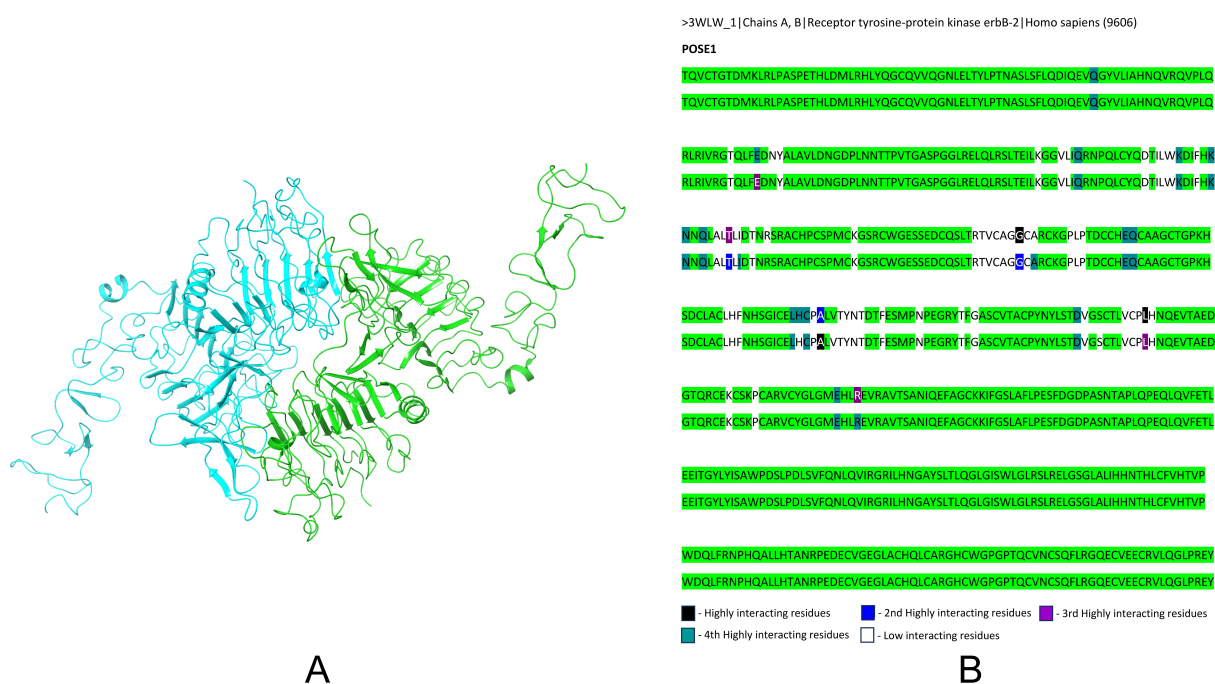
Figure 4. Dimerization of cancer HER2/ERBB2. (A) Dimerized structure of cancer cell HER2/ERBB2 (PDB ID 3WLW) – POSE1 (using Schrödinger Release 2023-4: BioLuminate, Schrödinger, LLC, New York, NY, 2023); and (B) record of interacting residues in cancer cell HER2/ERBB2 dimer structure obtained from Schrödinger software, where the pattern of colours represents strong to very strong interactions between the dimer

Comparative analysis

Sequential comparative analysis between normal and cancer HER2/ERBB2 using BLASTP and EMBOSS WATER revealed 99% and 99.6% identity, respectively, as shown in Figure 5. This high similarity indicates the presence of point mutations in the HER2/ERBB2 sequence in cancer cells. Secondary structure comparison using the PSIPRED tool showed shifts in loops, helices, and sheets in the cancer HER2/ERBB2 sequence compared to the normal HER2/ERBB2, as illustrated in Figure 6.

Finally, the 3D structures obtained from the PDB were compared by superposing them using Chimera software. Slight differences and shifts in protein folding were observed in the cancer cell HER2/ERBB2 structure compared to the normal cell HER2/ERBB2, as shown in Figure 7. These structural changes, caused by point mutations, result in the formation of strong homodimers in cancer cells, leading to the rapid activation of HER2/ERBB2 signaling and a significant increase in cell population.

```
A

Score            Expect  Method                        Identities      Positives      Gaps
1044 bits(2700)  0.0     Compositional matrix adjust.  506/508(99%)    508/508(100%)  0/508(0%)

Query  2    TQVCTGTDMKLRLPASPETHLDMLRHLYQGCQVVQGNLELTYLPTNASLSFLQDIQEVQG  61
            TQVCTGTDMKLRLPASPETHLDMLRHLYQGCQVVQGNLELTYLPTNASLSFLQDIQEVQG
Sbjct  1    TQVCTGTDMKLRLPASPETHLDMLRHLYQGCQVVQGNLELTYLPTNASLSFLQDIQEVQG  60

Query  62   YVLIAHNQVRQVPLQRLRIVRGTQLFEDNYALAVLDNGDPLNNTTPVTGASPGGLRELQL  121
            YVLIAHNQVRQVPLQRLRIVRGTQLFEDNYALAVLDNGDPLNNTTPVTGASPGGLRELQL
Sbjct  61   YVLIAHNQVRQVPLQRLRIVRGTQLFEDNYALAVLDNGDPLNNTTPVTGASPGGLRELQL  120

Query  122  RSLTEILKGGVLIQRNPQLCYQDTILWKDIFHKNNQLALTLIDTNRSRACHPCSPMCKGS  181
            RSLTEILKGGVLIQRNPQLCYQDTILWKDIFHKNNQLALTLIDTNRSRACHPCSPMCKGS
Sbjct  121  RSLTEILKGGVLIQRNPQLCYQDTILWKDIFHKNNQLALTLIDTNRSRACHPCSPMCKGS  180

Query  182  RCWGESSEDCQSLTRTVCAGGCARCKGPLPTDCCHEQCAAGCTGPKHSDCLACLHFNHSG  241
            RCWGESSEDCQSLTRTVCAGGCARCKGPLPTDCCHEQCAAGCTGPKHSDCLACLHFNHSG
Sbjct  181  RCWGESSEDCQSLTRTVCAGGCARCKGPLPTDCCHEQCAAGCTGPKHSDCLACLHFNHSG  240

Query  242  ICELHCPALVTYNTDTFESMPNPEGRYTFGASCVTACPYNYLSTDVGSCTLVCPLHNQEV  301
            ICELHCPALVTYNTDTFESMPNPEGRYTFGASCVTACPYNYLSTDVGSCTLVCPLHNQEV
Sbjct  241  ICELHCPALVTYNTDTFESMPNPEGRYTFGASCVTACPYNYLSTDVGSCTLVCPLHNQEV  300

Query  302  TAEDGTQKCEKCSKPCARVCYGLGMEHLREVRAVTSANIQEFAGCKKIFGSLAFLPESFD  361
            TAEDGTQ+CEKCSKPCARVCYGLGMEHLREVRAVTSANIQEFAGCKKIFGSLAFLPESFD
Sbjct  301  TAEDGTQRCEKCSKPCARVCYGLGMEHLREVRAVTSANIQEFAGCKKIFGSLAFLPESFD  360

Query  362  GDPASNTAPLQPEQLQVFETLEEITGYLYISAWPDSLPDLSVFQNLQVIRGRILHNGAYS  421
            GDPASNTAPLQPEQLQVFETLEEITGYLYISAWPDSLPDLSVFQNLQVIRGRILHNGAYS
Sbjct  361  GDPASNTAPLQPEQLQVFETLEEITGYLYISAWPDSLPDLSVFQNLQVIRGRILHNGAYS  420

Query  422  LTLQGLGISWLGLRSLRELGSGLALIHHNTHLCFVHTVPWDQLFRNPHQALLHTANRPED  481
            LTLQGLGISWLGLRSLRELGSGLALIHHNTHLCFVHTVPWDQLFRNPHQALLHTANRPED
Sbjct  421  LTLQGLGISWLGLRSLRELGSGLALIHHNTHLCFVHTVPWDQLFRNPHQALLHTANRPED  480

Query  482  ECVGEGLACHQLCAKGHCWGPGPTQCVN  509
            ECVGEGLACHQLCA+GHCWGPGPTQCVN
Sbjct  481  ECVGEGLACHQLCARGHCWGPGPTQCVN  508
```

```
B

# Length: 508
# Identity:     506/508 (99.6%)
# Similarity:   508/508 (100.0%)
# Gaps:           0/508 ( 0.0%)
# Score: 2787.0
#
#
#=======================================

EMBOSS_001    2  TQVCTGTDMKLRLPASPETHLDMLRHLYQGCQVVQGNLELTYLPTNASLS   51
                 ||||||||||||||||||||||||||||||||||||||||||||||||||
EMBOSS_002    1  TQVCTGTDMKLRLPASPETHLDMLRHLYQGCQVVQGNLELTYLPTNASLS   50

EMBOSS_001   52  FLQDIQEVQGYVLIAHNQVRQVPLQRLRIVRGTQLFEDNYALAVLDNGDP  101
                 ||||||||||||||||||||||||||||||||||||||||||||||||||
EMBOSS_002   51  FLQDIQEVQGYVLIAHNQVRQVPLQRLRIVRGTQLFEDNYALAVLDNGDP  100

EMBOSS_001  102  LNNTTPVTGASPGGLRELQLRSLTEILKGGVLIQRNPQLCYQDTILWKDI  151
                 ||||||||||||||||||||||||||||||||||||||||||||||||||
EMBOSS_002  101  LNNTTPVTGASPGGLRELQLRSLTEILKGGVLIQRNPQLCYQDTILWKDI  150

EMBOSS_001  152  FHKNNQLALTLIDTNRSRACHPCSPMCKGSRCWGESSEDCQSLTRTVCAG  201
                 ||||||||||||||||||||||||||||||||||||||||||||||||||
EMBOSS_002  151  FHKNNQLALTLIDTNRSRACHPCSPMCKGSRCWGESSEDCQSLTRTVCAG  200

EMBOSS_001  202  GCARCKGPLPTDCCHEQCAAGCTGPKHSDCLACLHFNHSGICELHCPALV  251
                 ||||||||||||||||||||||||||||||||||||||||||||||||||
EMBOSS_002  201  GCARCKGPLPTDCCHEQCAAGCTGPKHSDCLACLHFNHSGICELHCPALV  250

EMBOSS_001  252  TYNTDTFESMPNPEGRYTFGASCVTACPYNYLSTDVGSCTLVCPLHNQEV  301
                 ||||||||||||||||||||||||||||||||||||||||||||||||||
EMBOSS_002  251  TYNTDTFESMPNPEGRYTFGASCVTACPYNYLSTDVGSCTLVCPLHNQEV  300

EMBOSS_001  302  TAEDGTQKCEKCSKPCARVCYGLGMEHLREVRAVTSANIQEFAGCKKIFG  351
                 |||||||:|||||||||||||||||||||||||||||||||||||||||
EMBOSS_002  301  TAEDGTQRCEKCSKPCARVCYGLGMEHLREVRAVTSANIQEFAGCKKIFG  350

EMBOSS_001  352  SLAFLPESFDGDPASNTAPLQPEQLQVFETLEEITGYLYISAWPDSLPDL  401
                 ||||||||||||||||||||||||||||||||||||||||||||||||||
EMBOSS_002  351  SLAFLPESFDGDPASNTAPLQPEQLQVFETLEEITGYLYISAWPDSLPDL  400

EMBOSS_001  402  SVFQNLQVIRGRILHNGAYSLTLQGLGISWLGLRSLRELGSGLALIHHNT  451
                 ||||||||||||||||||||||||||||||||||||||||||||||||||
EMBOSS_002  401  SVFQNLQVIRGRILHNGAYSLTLQGLGISWLGLRSLRELGSGLALIHHNT  450

EMBOSS_001  452  HLCFVHTVPWDQLFRNPHQALLHTANRPEDECVGEGLACHQLCAKGHCWG  501
                 |||||||||||||||||||||||||||||||||||||||||:||||
EMBOSS_002  451  HLCFVHTVPWDQLFRNPHQALLHTANRPEDECVGEGLACHQLCARGHCWG  500

EMBOSS_001  502  PGPTQCVN  509
                 ||||||||
EMBOSS_002  501  PGPTQCVN  508
```

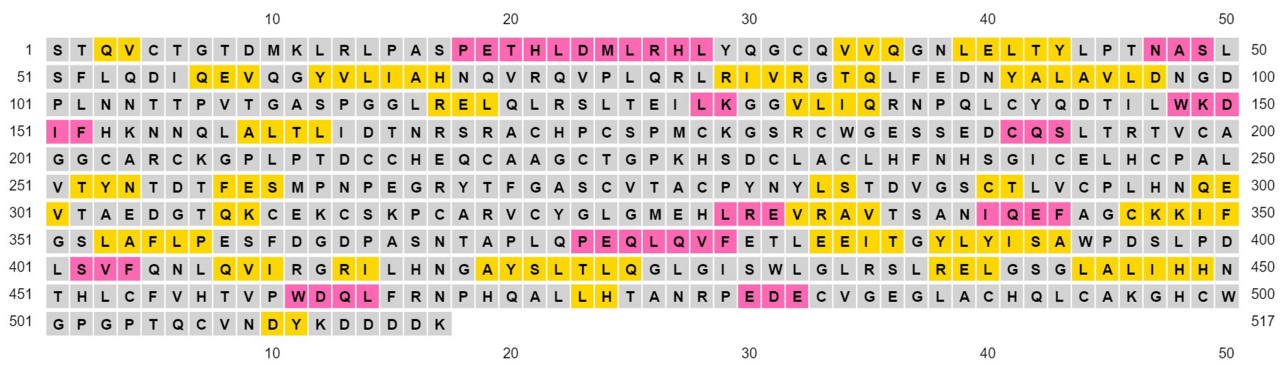A   B

Figure 5. Sequential comparative analysis. (A) Using NCBI BLASTP showing 99% identity between normal and cancer cell HER2/ERBB2 sequence; and (B) using EMBOSS WATER, 99.6% identity found between normal and cancer cell HER2/ERBB2 sequence indicating point mutations in certain regions of the FASTA sequence
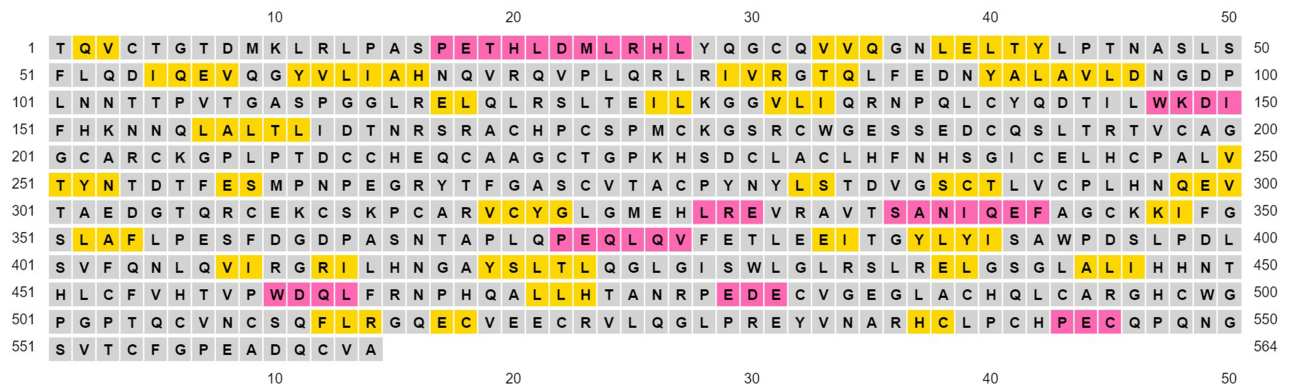
Discussion

The comprehensive analysis delineates a stark contrast between the dimerization capabilities of HER2/ERBB2 in normal and cancerous cells. In normal cells, HER2/ERBB2 struggles to form stable homodimers and the identification of only 12 interacting residues, underscoring the protein's inability to engage in substantial interactions necessary for stable dimer formation (Table 3). This finding is pivotal as it highlights the inherent stability issues within the normal HER2/ERBB2 homodimers, suggesting a natural regulatory mechanism that prevents the activation of cell proliferative signaling pathways. Conversely, in cancerous cells, HER2/ERBB2 demonstrates a remarkable ability to form stable homodimers and a robust network of 165 interacting residues (Table 3). This stark contrast underpins the pathogenic potency of cancerous HER2/ERBB2, as these stable homodimers relentlessly activate cell proliferation signaling, leading to uncontrolled cell growth. The near-identical sequence homology between normal and cancerous HER2/ERBB2, with single point mutations, yet profound differences in dimerization capabilities, underscores the critical role of structural nuances in protein function and disease progression. These findings beckon a deeper exploration of the structural and functional dynamics of HER2/ERBB2, offering potential avenues for therapeutic intervention aimed at destabilizing these pathogenic homodimers in cancerous cells, thereby mitigating the aggressive proliferation characteristic of cancer.

Overall, the structural characterization of HER2/ERBB2 proteins underscores the pivotal role of dimerization and interaction strength in modulating the signaling cascades that drive cell proliferation. These findings offer valuable insights into the molecular mechanisms underlying HER2/ERBB2-mediated carcinogenesis, emphasizing how alterations in protein structure and interactions can lead to uncontrolled cell growth and cancer progression. This knowledge is crucial for developing targeted therapies for HER2/ERBB2-positive cancers, where interrupting or modulating these interactions could effectively inhibit tumor growth.

A

B

Strand   Helix   Coil   Disordered

Disordered, protein binding   Putative Domain Boundary   Membrane Interaction   Transmembrane Helix

Extracellular   Re-entrant Helix   Cytoplasmic   Signal Peptide

Figure 6. Secondary structure prediction of (A) normal cell HER2/ERBB2 (PDB ID 2A91); and (B) cancer cell HER2/ERBB2 (PDB ID 3WLW), using their FASTA sequence as input in PSIPRED tool

Figure 7. Comparative analysis by superposing both HER2/ERBB2 and visualizing their 3D structure using UCSF Chimera software

Table 3. Summary of result analysis

Feature	Normal cell HER2/ERBB2	Cancer cell HER2/ERBB2
Number of dimerized structures obtained	12	15
PIPER pose energy score (best docking score)	−133.7 (No score above −900)	−1,238.94 (Scores above −900)
Number of interacting residues	12	165
Stability of homodimers	No stable dimer found	Stable dimer structures obtained
Interaction analysis in Schrödinger	Unable to perform due to weak interactions	Conducted successfully, showing strong to very strong interactions
Sequence identity (BLASTP)	-	99% similarity with normal HER2/ERBB2
Sequence identity (EMBOSS WATER)	-	99.6% similarity with normal HER2/ERBB2
Secondary structure comparison (PSIPRED)	-	Shift in loops, helices, and sheets observed compared to normal HER2/ERBB2
3D structure comparison (Chimera)	-	Slight difference and shift in protein folding compared to normal HER2/ERBB2

The analysis revealed that even single-point mutations in non-active regions of HER2/ERBB2 can induce significant alterations in the overall protein architecture. This phenomenon is critical because it demonstrates that mutations outside the active site can still have profound effects on protein function by altering its folding, stability, and interaction capabilities. Such structural changes can enhance the protein's ability to form stable homodimers, as observed in cancer cells, leading to the continuous activation of proliferative signaling pathways.

These insights have substantial implications for drug discovery and development. Traditional molecular docking and dynamics simulations often focus predominantly on the active sites of target proteins, aiming to identify compounds that can effectively bind and inhibit these regions. However, the findings from this study highlight the necessity of considering the entire protein structure in drug design strategies. By accounting for potential conformational changes induced by mutations outside the active site, researchers can develop more effective therapeutic agents that target the protein's overall architecture and interaction networks.

Moreover, this comprehensive approach can help identify allosteric sites and secondary binding pockets that could be exploited for therapeutic intervention. Allosteric modulators, which bind to regions other than the active site, can induce conformational changes that affect the protein's activity and interactions. This strategy could provide a more nuanced and effective means of regulating HER2/ERBB2 function and mitigating its role in cancer.

In summary, the structural characterization of HER2/ERBB2 proteins not only enhances our understanding of HER2/ERBB2-mediated carcinogenesis but also informs the development of more sophisticated and effective targeted therapies. By considering the entire protein structure and the impact of mutations beyond the active site, researchers can better design drugs that address the complex molecular dynamics of HER2/ERBB2 and similar oncogenic proteins. This holistic approach holds promise for improving therapeutic outcomes in HER2/ERBB2-positive cancers and potentially other diseases driven by similar molecular mechanisms.

A limitation of this study is that we were able to analyze only a single protein structure and its related pathways. For a more comprehensive understanding, it is essential to explore additional protein structures and associated pathways. Furthermore, these findings need to be validated under in vivo conditions to confirm their relevance and applicability in a physiological context.

Abbreviations

CDC37: cell division cycle 37

EGFR: epidermal growth factor receptor

HER2/ERBB2: v-erb-b2 avian erythroblastic leukemia viral oncogene homolog 2

HSP90: heat shock protein 90

IRF3: interferon regulatory factor 3

MAVS: mitochondrial antiviral-signaling protein

MLKL: mixed lineage kinase domain-like protein

PDB: Protein Data Bank

RIPK3: receptor-interacting protein kinase-3

TBK1: TANK-binding kinase 1

Supplementary materials

The supplementary figures for this article are available at: https://www.explorationpub.com/uploads/Article/file/1001237_sup_1.pdf.

Declarations

Acknowledgments

Author contributions

JS: Methodology, Investigation, Writing—original draft. PM: Conceptualization, Methodology, Investigation, Supervision, Writing—review & editing. HV: Formal analysis, Writing—review & editing. All authors read and approved the submitted version.

Conflicts of interest

The authors declare that they have no conflicts of interest.

Ethical approval

Not applicable.

Consent to participate

Not applicable.

Consent to publication

Not applicable.

Availability of data and materials

The raw data supporting the conclusions of this manuscript will be made available by the authors, without undue reservation, to any qualified researcher.

Funding

Copyright

References

1. Hu S, Sun Y, Meng Y, Wang X, Yang W, Fu W, et al. Molecular architecture of the ErbB2 extracellular domain homodimer. Oncotarget. 2015;6:1695–706. [DOI] [PubMed] [PMC]

2. Li E, Hristova K. Role of receptor tyrosine kinase transmembrane domains in cell signaling and human pathologies. Biochemistry. 2006;45:6241–51. [DOI] [PubMed] [PMC]

3. Franklin MC, Carey KD, Vajdos FF, Leahy DJ, Vos AMd, Sliwkowski MX. Insights into ErbB signaling from the structure of the ErbB2-pertuzumab complex. Cancer Cell. 2004;5:317–28. [DOI] [PubMed]

4. Landgraf R. HER2 therapy. HER2 (ERBB2): functional diversity from structurally conserved building blocks. Breast Cancer Res. 2007;9:202. [DOI] [PubMed] [PMC]

5. Furrer D, Paquet C, Jacob S, Diorio C. The Human Epidermal Growth Factor Receptor 2 (HER2) as a Prognostic and Predictive Biomarker: Molecular Insights into HER2 Activation and Diagnostic Implications. In: Lemamy GJ, editor. Cancer Prognosis. IntechOpen; 2018.

6. Rubin I, Yarden Y. The basic biology of HER2. Ann Oncol. 2001;12 Suppl 1:S3–8. [DOI] [PubMed]

7. Xu W, Yuan X, Beebe K, Xiang Z, Neckers L. Loss of Hsp90 association up-regulates Src-dependent ErbB2 activity. Mol Cell Biol. 2007;27:220–8. [DOI] [PubMed] [PMC]

8. Borg JP, Marchetto S, Bivic AL, Ollendorff V, Jaulin-Bastard F, Saito H, et al. ERBIN: a basolateral PDZ protein that interacts with the mammalian ERBB2/HER2 receptor. Nat Cell Biol. 2000;2:407–14. [DOI] [PubMed]

9. Citri A, Gan J, Mosesson Y, Vereb G, Szollosi J, Yarden Y. Hsp90 restrains ErbB-2/HER2 signalling by limiting heterodimer formation. EMBO Rep. 2004;5:1165–70. [DOI] [PubMed] [PMC]

10. Du Z, Lovly CM. Mechanisms of receptor tyrosine kinase activation in cancer. Mol Cancer. 2018;17:58. [DOI] [PubMed] [PMC]

11. Hazan R, Margolis B, Dombalagian M, Ullrich A, Zilberstein A, Schlessinger J. Identification of autophosphorylation sites of HER2/neu. Cell Growth Differ. 1990;1:3–7.

12. Pickl M, Ries CH. Comparison of 3D and 2D tumor models reveals enhanced HER2 activation in 3D associated with an increased response to trastuzumab. Oncogene. 2009;28:461–8. [DOI] [PubMed]

13. Ricci A, Lanfrancone L, Chiari R, Belardo G, Pertica C, Natali PG, et al. Analysis of protein-protein interactions involved in the activation of the Shc/Grb-2 pathway by the ErbB-2 kinase. Oncogene. 1995;11:1519–29. [PubMed]

14. Gillespie M, Jassal B, Stephan R, Milacic M, Rothfels K, Senff-Ribeiro A, et al. The reactome pathway knowledgebase 2022. Nucleic Acids Res. 2022;50:D687–92. [DOI] [PubMed] [PMC]

15. Li T, Jiang H, Tong Y, Lu J. Targeting the Hsp90-Cdc37-client protein interaction to disrupt Hsp90 chaperone machinery. J Hematol Oncol. 2018;11:59. [DOI] [PubMed] [PMC]

16. Ricci AD, Rizzo A, Llimpe FLR, Fabio FD, Biase DD, Rihawi K. Novel HER2-Directed Treatments in Advanced Gastric Carcinoma: AnotHER Paradigm Shift? Cancers (Basel). 2021;13:1664. [DOI] [PubMed] [PMC]

17. Rizzo A, Cusmai A, Acquafredda S, Rinaldi L, Palmiotti G. Ladiratuzumab vedotin for metastatic triple negative cancer: preliminary results, key challenges, and clinical potential. Expert Opin Investig Drugs. 2022;31:495–8. [DOI] [PubMed]

18. Quagliariello V, Laurentiis MD, Cocco S, Rea G, Bonelli A, Caronna A, et al. NLRP3 as Putative Marker of Ipilimumab-Induced Cardiotoxicity in the Presence of Hyperglycemia in Estrogen-Responsive and Triple-Negative Breast Cancer Cells. Int J Mol Sci. 2020;21:7802. [DOI] [PubMed] [PMC]

19. Berman HM, Westbrook J, Feng Z, Gilliland G, Bhat TN, Weissig H, et al. The Protein Data Bank. Nucleic Acids Res. 2000;28:235–42. [DOI] [PubMed] [PMC]

20. Beard H, Cholleti A, Pearlman D, Sherman W, Loving KA. Applying physics-based scoring to calculate free energies of binding for single amino acid mutations in protein-protein complexes. PLoS One. 2013;8:e82849. [DOI] [PubMed] [PMC]

21. Salam NK, Adzhigirey M, Sherman W, Pearlman DA. Structure-based approach to the prediction of disulfide bonds in proteins. Protein Eng Des Sel. 2014;27:365–74. [DOI] [PubMed]

22. Zhu K, Day T, Warshaviak D, Murrett C, Friesner R, Pearlman D. Antibody structure determination using a combination of homology modeling, energy-based refinement, and loop prediction. Proteins. 2014;82:1646–55. [DOI] [PubMed] [PMC]

23. Sastry GM, Adzhigirey M, Day T, Annabhimoju R, Sherman W. Protein and ligand preparation: parameters, protocols, and influence on virtual screening enrichments. J Comput Aided Mol Des. 2013; 27:221–34. [DOI] [PubMed]

24. Chuang GY, Kozakov D, Brenke R, Comeau SR, Vajda S. DARS (Decoys As the Reference State) potentials for protein-protein docking. Biophys J. 2008;95:4217–27. [DOI] [PubMed] [PMC]

25. Fernández-Recio J, Sternberg MJE. The 4th meeting on the Critical Assessment of Predicted Interaction (CAPRI) held at the Mare Nostrum, Barcelona. Proteins. 2010;78:3065–6. [DOI]

26. Kozakov D, Brenke R, Comeau SR, Vajda S. PIPER: an FFT-based protein docking program with pairwise potentials. Proteins. 2006;65:392–406. [DOI] [PubMed]

27. Altschul SF, Gish W, Miller W, Myers EW, Lipman DJ. Basic local alignment search tool. J Mol Biol. 1990;215:403–10. [DOI] [PubMed]

28. Madeira F, Pearce M, Tivey ARN, Basutkar P, Lee J, Edbali O, et al. Search and sequence analysis tools services from EMBL-EBI in 2022. Nucleic Acids Res. 2022;50:W276–9. [DOI] [PubMed] [PMC]

29. McGuffin LJ, Bryson K, Jones DT. The PSIPRED protein structure prediction server. Bioinformatics. 2000;16:404–5. [DOI] [PubMed]

30. Pettersen EF, Goddard TD, Huang CC, Couch GS, Greenblatt DM, Meng EC, et al. UCSF Chimera--a visualization system for exploratory research and analysis. J Comput Chem. 2004;25:1605–12. [DOI] [PubMed]

31. Boyault C, Zhang Y, Fritah S, Caron C, Gilquin B, Kwon SH, et al. HDAC6 controls major cell response pathways to cytotoxic accumulation of protein aggregates. Genes Dev. 2007;21:2172–81. [DOI] [PubMed] [PMC]

32. Bublik DR, Scolz M, Triolo G, Monte M, Schneider C. Human GTSE-1 regulates p21$^{CIP1/WAF1}$ stability conferring resistance to paclitaxel treatment. J Biol Chem. 2010;285:5274–81. [DOI] [PubMed] [PMC]

33. Jascur T, Brickner H, Salles-Passador I, Barbier V, Khissiin AE, Smith B, et al. Regulation of p21$^{WAF1/CIP1}$ stability by WISp39, a Hsp90 binding TPR protein. Mol Cell. 2005;17:237–49. [DOI] [PubMed]

34. Yu D, Jing T, Liu B, Yao J, Tan M, McDonnell TJ, et al. Overexpression of ErbB2 blocks Taxol-induced apoptosis by upregulation of p21^{Cip1}, which inhibits p34^{Cdc2} kinase. Mol Cell. 1998;2:581–91. [DOI] [PubMed]

35. Zou J, Guo Y, Guettouche T, Smith DF, Voellmy R. Repression of heat shock transcription factor HSF1 activation by HSP90 (HSP90 complex) that forms a stress-sensitive complex with HSF1. Cell. 1998;94: 471–80. [DOI] [PubMed]

36. Roe SM, Ali MMU, Meyer P, Vaughan CK, Panaretou B, Piper PW, et al. The Mechanism of Hsp90 regulation by the protein kinase-specific cochaperone p50^{cdc37}. Cell. 2004;116:87–98. [DOI] [PubMed]

37. Liu X, Wei B, Shi H, Shan Y, Wang C. Tom70 mediates activation of interferon regulatory factor 3 on mitochondria. Cell Res. 2010;20:994–1011. [DOI] [PubMed]

38. Yang K, Shi H, Qi R, Sun S, Tang Y, Zhang B, et al. Hsp90 regulates activation of interferon regulatory factor 3 and TBK-1 stabilization in Sendai virus-infected cells. Mol Biol Cell. 2006;17:1461–71. [DOI] [PubMed] [PMC]

39. Bigenzahn JW, Fauster A, Rebsamen M, Kandasamy RK, Scorzoni S, Vladimer GI, et al. An Inducible Retroviral Expression System for Tandem Affinity Purification Mass-Spectrometry-Based Proteomics Identifies Mixed Lineage Kinase Domain-like Protein (MLKL) as an Heat Shock Protein 90 (HSP90) Client. Mol Cell Proteomics. 2016;15:1139–50. [DOI] [PubMed] [PMC]

40. Jacobsen AV, Lowes KN, Tanzer MC, Lucet IS, Hildebrand JM, Petrie EJ, et al. HSP90 activity is required for MLKL oligomerisation and membrane translocation and the induction of necroptotic cell death. Cell Death Dis. 2016;7:e2051. [DOI] [PubMed] [PMC]

41. Zhao XM, Chen Z, Zhao JB, Zhang PP, Pu YF, Jiang SH, et al. Hsp90 modulates the stability of MLKL and is required for TNF-induced necroptosis. Cell Death Dis. 2016;7:e2089. [DOI] [PubMed] [PMC]

42. Li D, Xu T, Cao Y, Wang H, Li L, Chen S, et al. A cytosolic heat shock protein 90 and cochaperone CDC37 complex is required for RIP3 activation during necroptosis. Proc Natl Acad Sci U S A. 2015;112: 5017–22. [DOI] [PubMed] [PMC]